Received: 8 November 2018 | Revised: 23 December 2019 | Accepted: 2 March 2020
DOI: 10.1002/asl.967

RESEARCH ARTICLE

Atmospheric Science Letters RMetS

On the evidence of orographical modulation of regional fine scale precipitation change signals: The Carpathians

Csaba Torma[1] | **Filippo Giorgi**[2]

[1]Department of Meteorology, Eötvös Loránd University and MTA Post-Doctoral Research Program, Budapest, Hungary

[2]Earth System Physics Section, The Abdus Salam International Centre for Theoretical Physics, Trieste, Italy

Correspondence
Csaba Torma, Department of Meteorology, Eötvös Loránd University and MTA Post-Doctoral Research Program, Pázmány Péter st. 1/A, H-1117 Budapest, Hungary.
Email: tcsabi@caesar.elte.hu

Funding information
Magyar Tudományos Akadémia, Grant/Award Number: BO/639/19; Ministry for Innovation and Technology, Grant/Award Number: ÚNKP-19-4-ELTE-1202

Abstract
This study investigates the greenhouse gas-induced winter and summer precipitation change signals over the Carpathian region with special focus on topographical effects and underlying processes. Six high-resolution (~12 km grid spacing) regional climate model projections are analyzed for the future period 2070–2099 with respect to the reference period 1976–2005 under the RCP8.5 scenarios. We find that the topographically induced fine scale modulation of the precipitation change signal is mostly of dynamical nature in winter (due to the precipitation shadowing effect), and thermodynamical in summer (associated with high elevation convection) over the region of interest. Additionally, elevation, size, and orientation of mountains play key roles in such processes. Our results draw attention to the fact that the high-resolution representation of topography in climate models is crucial for the provision of fine scale precipitation projections in mountainous regions.

KEYWORDS
Carpathian climate, precipitation change, regional climate modeling

1 | INTRODUCTION

The Carpathian Basin lies in Central-eastern Europe, east of the Alpine region, and extends between 44°–50° north and 17°–27° east. Its main morphological features include the Hungarian Plain surrounded to its north, east, and southern flanks by the Carpathian mountain range, with an altitude range between 27 and 2,655 m (Figure S1). The Carpathians play an important role for the climate of the Basin (e.g., by blocking cold air masses from the north), where typically the warm dry air of the Balkans meets the temperate Central Europe and cold continental Eastern Europe flow (UNEP, 2007). Oceanic, continental, and Mediterranean effects, as well as orographic factors, characterize the climate of the Carpathian basin, which hosts a rich biosphere (Kuemmerle *et al.*, 2010) in terms of forests, meadows, and crop fields (Bálint *et al.*, 2011). Therefore, investigating climate variability and the possible effects of climate change on water resources over the Carpathian Basin is essential (Kozak *et al.*, 2011).

The complex morphology of the Basin, and in particular the Carpathian Mountains, can be expected to substantially modulate the local climate change signal. Previous studies have shown that regional precipitation change patterns can be substantially modulated by topography, either through the precipitation shadowing effect (e.g., Giorgi *et al.*, 1994; Gao *et al.*, 2006) or through the generation of convective instability at high elevations (Giorgi *et al.*, 2016). However, these processes depend substantially on the prevailing wind flows and on the characteristics of topography, such as elevation and slope, and thus on the resolution at which these characteristics are represented in climate models.

The high-resolution regional climate model (RCM) projections for the European region completed as part of the EURO-CORDEX (Jacob *et al.*, 2014) and Med-CORDEX (Ruti *et al.*, 2016) initiatives provide an optimal dataset to explore the issue of the effects of the Carpathians on the regional precipitation change signal. Therefore, in this study, we present such an analysis, with the particular aim of identifying similarities and differences compared to what found, for example, for the Alpine region (Gao *et al.*, 2006; Giorgi *et al.*, 2016), which has distinctly different characteristics from the Carpathians in terms of elevation and slope.

In this regard, we focus separately on the winter and summer seasons because the processes underlying precipitation formation are different. While in the winter precipitation is mostly associated with the occurrence of Atlantic systems traveling eastward over the region and impinging upon the Carpathians, in the summer local convection plays a more dominant role.

2 | EXPERIMENT DESIGN AND ANALYSIS TECHNIQUE

The region of interest encompasses the Carpathian Basin and is shown in Figure S1. The figure also presents the topography of the Carpathian chain at the resolution of the RCMs analyzed (grid spacing resolution of 0.11°, or ~12 km) and from the very high-resolution (1′) GTOPO30 database. It can be seen that at 12 km resolution, the main features of the Carpathians are captured, albeit in a somewhat smoothed way, with topographic maxima reaching 1,500 (up to 2,200 m in the GTOPO dataset) and with mountain chains extending in both the north–south and east–west directions. Note that this region is included in the interior of both the EURO-CORDEX and Med-CORDEX domains, thus ideal for using RCM simulations from both initiatives (Figure S1).

We analyzed the mini ensemble of six RCM simulations shown in Table 1, which is the same used by Giorgi *et al.* (2016) for the Alpine region and was obtained from the EURO-CORDEX and Med-CORDEX datasets. Note that the ensemble includes only individual RCM simulations, even though different global climate model (GCM)-driven simulations are available for some of the RCMs, in order not to have a specific RCM dominate the ensemble. Table 1 also shows the GCMs driving the RCM experiments. We analyze the December–January–February (DJF, winter) and June–July–August (JJA, summer) seasons for the late 21st century 30-year time slice 2070–2099 compared to the reference period 1976–2005 in the high end RCP8.5 scenario (Moss *et al.*, 2010). This was done in order to maximize the signal, noting however that similar conclusions hold for earlier time slices (not shown for brevity).

TABLE 1 Overview of global and regional climate models used in the present study. For the regional models, the letter in parenthesis indicates the driving GCM (from CMIP5) and whether the run uses the EURO-CORDEX (EC) or Med-CORDEX (MC) domain

Model	Modeling group	Horizontal resolution
(a) CNRM-CM5 (Voldoire *et al.*, 2012)	Centre National de Recherches Meteorologiques and Centre Europeen de Recherches et de formation Avancee en Calcul Scientifique, France	1.40625° × 1.40625°
(b) EC-EARTH (Hazeleger *et al.*, 2010)	Irish Centre for High-end Computing, Ireland	1.125° × 1.125°
(c) HadGEM2-ES (Collins *et al.*, 2011)	Met Office Hadley Centre, UK	1.875° × 1.2413°
(d) MPI-ESM-LR (Jungclaus *et al.*, 2010)	Max Planck Institute for Meteorology, Germany	1.875° × 1.875°
ALADIN (a-MC) (Colin *et al.*, 2010)	Centre National de Recherches Meteorologiques, France	0.11°
CCLM (d-EC) (Rockel *et al.*, 2008)	Climate limited-area modeling community, Germany	0.11°
RCA4 (c-EC) (Kupiainen *et al.*, 2014)	Swedish Meteorological and Hydrological Institute, Rossby Centre, Sweden	0.11°
RACMO (b-EC) (Meijgaard et al., 2012)	Royal Netherlands Meteorological Institute, the Netherlands	0.11°
REMO (d-EC) (Jacob *et al.*, 2001)	Max-Planck-Institut für Meteorologie, Germany	0.11°
RegCM4 (c-MC) (Giorgi *et al.*, 2012)	International Centre for Theoretical Physics, Italy	0.11°

Figure S2 presents a comparison of ensemble averaged simulated precipitation by the RCM and driving GCM ensembles with the observations of CARPATCLIM (Szalai *et al.*, 2013). It shows that the RCM ensemble is able to capture the topographically induced precipitation patterns over the region and considerably improves these patterns compared to the driving GCMs. Note that the original CARPATCLIM dataset does not include corrections for wind-induced undercatch by precipitation gauges. Thus, following the work of Torma et al. (2015), an additional monthly based undercatch correction obtained from the global precipitation dataset of the University of Delaware (Legates and Willmott, 1990) was applied to the CARPATCLIM data.

3 | PRECIPITATION CHANGE PATTERNS

Figure 1 shows the ensemble average DJF and JJA precipitation change patterns (2070–2099 minus 1976–2005) over the Carpathian region for the driving GCM and nested RCM ensembles. As found in previous generations of models, at the large scale the region experiences a general increase in precipitation during the winter season and a decrease during summer (e.g., Déqué *et al.*, 2007; Giorgi and Coppola, 2010; Jacob *et al.*, 2014). In the RCMs, this pattern is evidently inherited by the driving GCMs. In both the winter and summer, however, significant differences can be found between the two ensembles, in particular related to the presence of the Carpathian chain.

We first focus on the winter season. Figure 1 shows a maximum increase in the western portion of the basin, predominantly flat, both in the GCM and RCM ensemble, although more marked in the latter. While however the precipitation enhancement tends to decrease toward the east in the GCMs, we can observe maxima in correspondence of the mountain chains in the RCMs, and specifically over the eastern flanks of the Outer Eastern Carpathians and the northern flanks of the Southern Carpathians.

To investigate the origin of these maxima, Figure 2 presents the change in DJF precipitation and 850 hPa wind for each individual GCM/RCM pair along with the corresponding "downscaling signal", or DS, introduced by Giorgi *et al.* (2016). The DS is defined as the local difference between RCM and GCM precipitation change after the area mean change is removed (to remove systematic differences across the two models), that is, it is a measure of the fine scale modulation of the signal by the RCMs.

First, it can be seen that even though the Carpathian Basin lies toward the center of the RCM domains, the change in regional scale wind is mostly driven by the GCMs, although with some modulation by the corresponding RCMs, especially in the case of the HadGEM/RCA4 pair. The figure shows a close correspondence between the RCM-produced precipitation change, change in mean wind direction, and orientation of the mountain chain (which determines the sign of the precipitation shadowing effect). This is especially evident when analyzing the DS. In the CNRM-CM5/ALADIN and HadGEM/RegCM pairs, the change in flow is mostly from the northerly direction, resulting in a positive DS

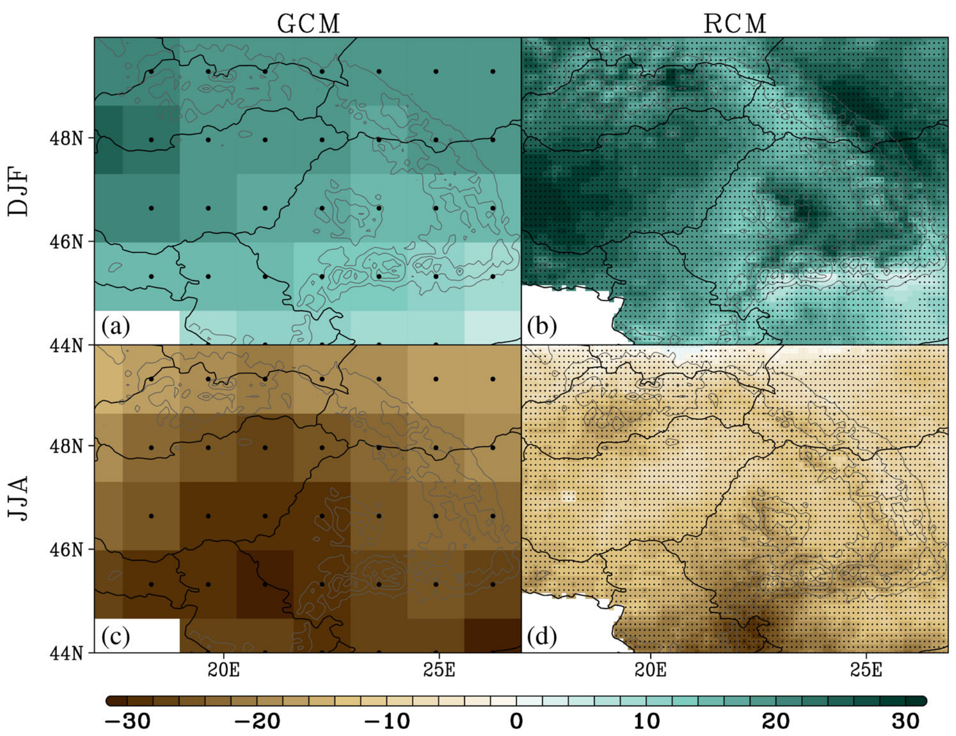

FIGURE 1 Ensemble average of GCM and RCM projected percent change in winter and summer precipitation over the Carpathian region for the future time slice 2070–2099 compared to the reference period 1976–2005. Panel (a) GCM ensemble, 2070–2099 (DJF); (b) RCM ensemble, 2070–2099 (DJF); (c) GCM ensemble, 2070–2099 (JJA); (d) RCM ensemble, 2070–2099 (JJA). Dotting indicates areas where at least 3 out of 4 GCMs or 4 out of 6 RCMs agree on the sign of the signal. Thin contour lines represent topography with intervals of 500 m

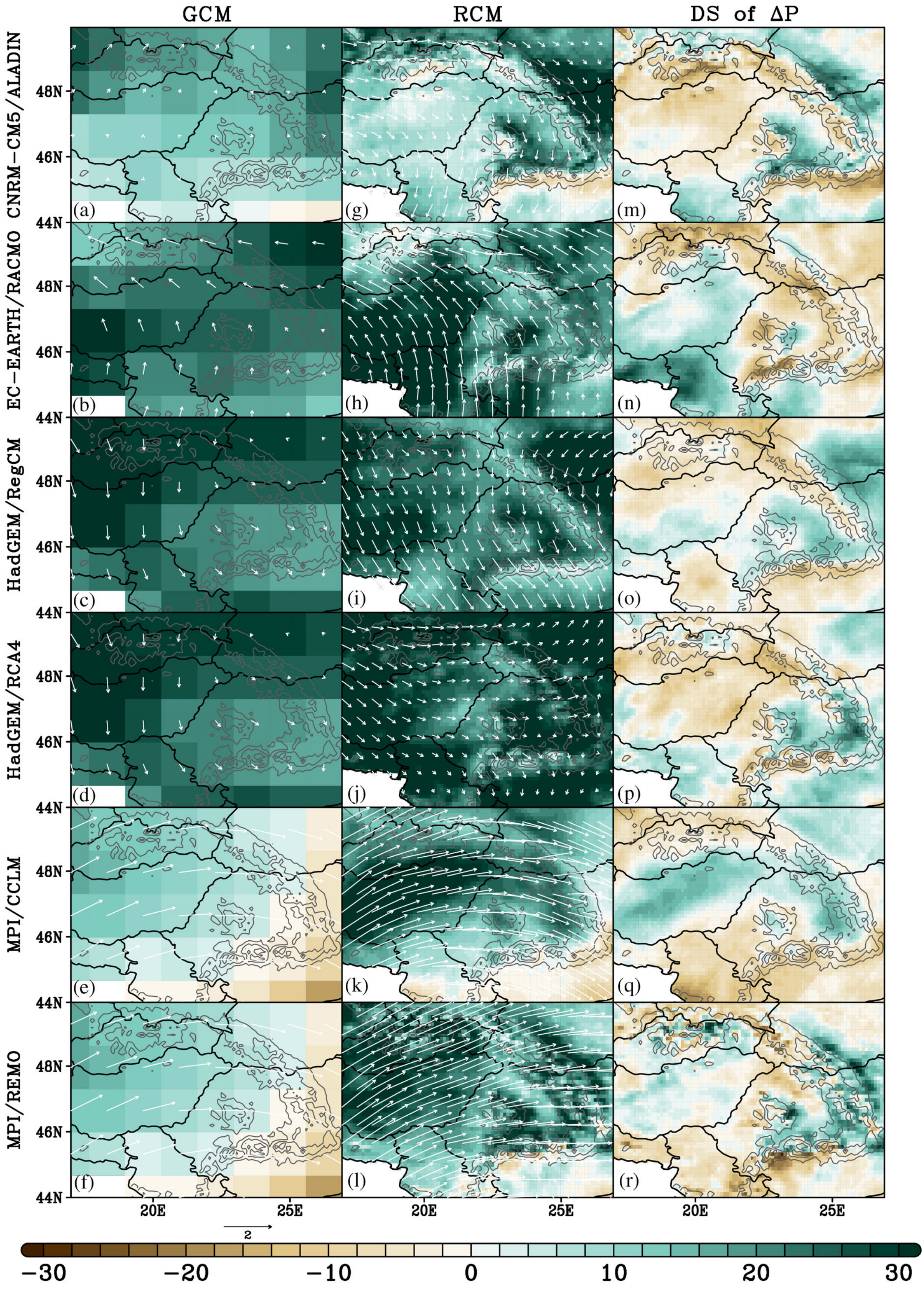

FIGURE 2 Changes in mean winter (DJF) precipitation along with the change in 850 hPa wind field for each individual GCM/RCM pair along with the corresponding "downscaling signal", or DS for 2070–2099 compared to the reference period 1976–2005. Precipitation change and DS are given in percentage, while the 850 hPa wind field changes are given in ms^{-1}. Thin contour lines represent topography with intervals of 500 m

(increased change) along the northern and northeastern (upwind) flanks of the mountain chains. Conversely, in the HadGEM/RCA4 and MPI/CCLM, the change in flow is mostly from the west, resulting positive DS along the western topographic slopes. In the EC-EARTH/RACMO pair the change in flow is mostly southeasterly, parallel to the main orientation of the chain and thus the DS is not large. Finally, in the MPI/REMO pair, we find positive DS both in the eastern and western mountain slopes even though the prevailing mean wind change is from the west. Evidently, in this case, the interannual variability of wind change is an important element contributing to the precipitation change.

In summary, Figure 2 shows that a key factor determining the regional spatial distribution of the winter precipitation change signal over the Carpathian region by the end of the 21st century is the orientation of the mountain chains with respect to the main flow change, which in turn determines the intensity of the precipitation shadowing effect. In other words, the topographically induced signal is mostly of dynamical nature.

Moving now to the summer season, here the effect has a more thermodynamic origin. Figure 3 shows the ensemble average of summer precipitation change in the GCM and RCM ensembles, along with the change in convective and resolvable scale precipitation and the DS of the ensemble average change. At the large scale, there is a maximum in precipitation decrease over the southern portion of the basin in both ensembles, whose center is however slightly shifted across the two datasets. The DS shows a positive anomaly over the Hungarian plains (i.e., a lower reduction of precipitation in the RCMs) mostly tied to the resolvable scale component of rainfall, which actually shows an increase there. Comparison with the change in convective precipitation, which is strongly negative, would indicate some shift of precipitation mode from convective to non-convective. Figure S3 shows the precipitation and 850 hPa wind changes and the DS for each individual GCM/RCM pair for the summer (JJA).

The effect of topography, however, can be mostly seen in the convective precipitation change field, where throughout the highest mountain peaks convection

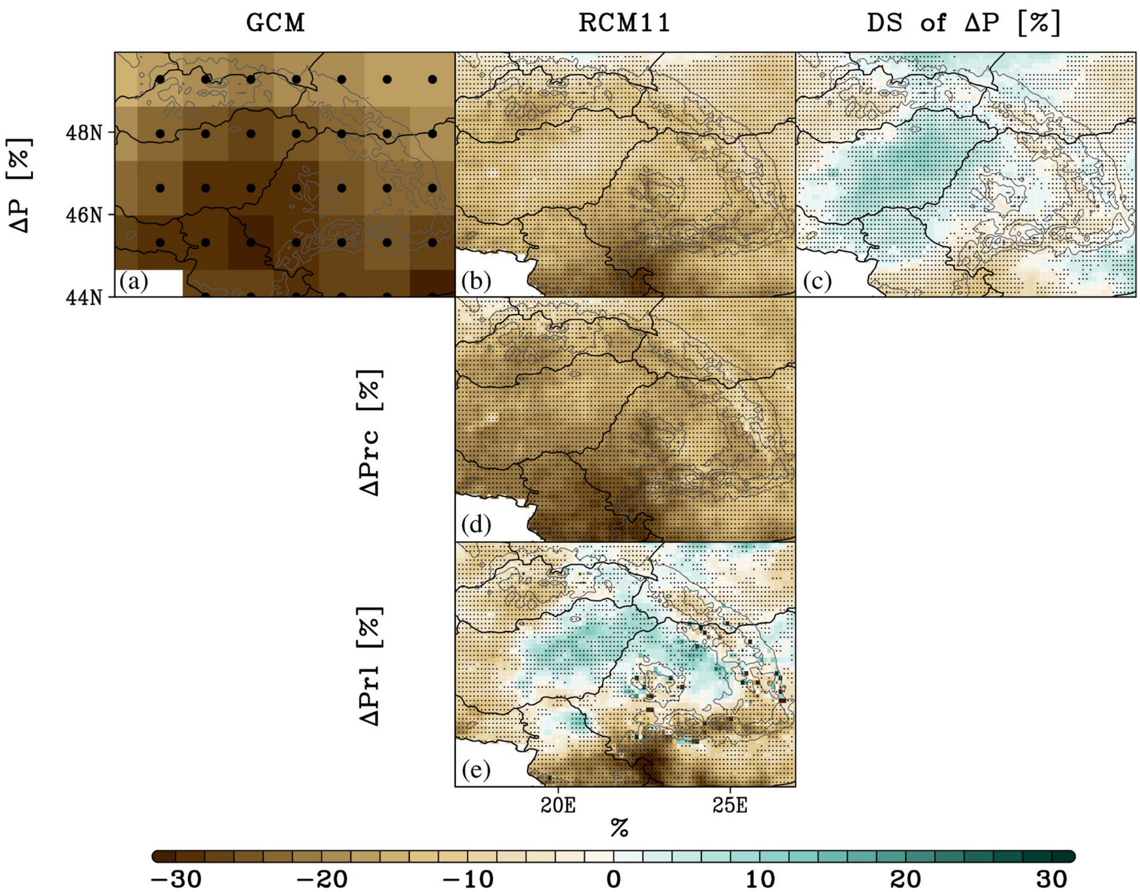

FIGURE 3 Ensemble average percent change in summer precipitation (2070–2099 vs. 1976–2005) in the GCM (panel a) and RCM ensembles (panel b), along with the change in convective (panel d) and resolvable scale precipitation (panel e) and the DS of the ensemble average change (panel c). Dotting indicates areas where at least 3 out of 4 GCMs or 4 out of 6 RCMs agree on the sign of the signal. Thin contour lines represent topography with intervals of 500 m

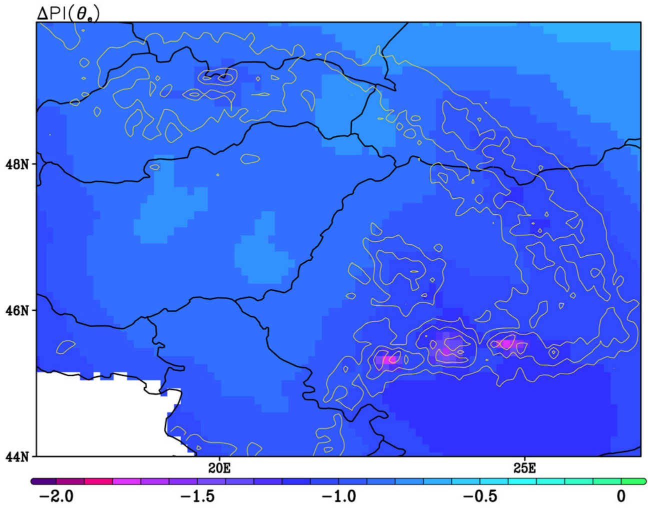

FIGURE 4 Change in summer mean potential instability index with inclusion of moisture. Units are °C. Thin contour lines represent topography with intervals of 500 m

shows a less marked decrease and the precipitation DS show small but positive values. This is due to a maximum increase in potential for convection as measured by the potential instability index, defined as the difference between equivalent potential temperature at 500 and 850 hPa. Higher negative values of the index imply greater potential for convection, and the large decreases of this index occurring over the highest peaks of the Carpathian Mountains (Figure 4) are indications of increases in convection potential associated with high elevation heating. We found this signal quite robust as most models agreed on the sign of the change all over the region of interest. This process is similar to that found by Giorgi *et al.* (2016) over the Alpine region, with the important difference that while over the Alps it was sufficient to reverse the precipitation change signal over the mountain tops from negative to positive, here it only attenuates the precipitation reduction. This indicates that this process is strongly dependent on elevation and the extent of the mountainous areas.

4 | DISCUSSION AND SUMMARY CONSIDERATIONS

In this paper, we analyzed the topographically induced fine scale seasonal precipitation change signal in high-resolution RCM projections over the Carpathian region by the end of the 21st century (2070–2099). We found that the Carpathian Mountains significantly affect precipitation change patterns both in winter and summer, but with different underlying mechanisms. In the winter, the topographic forcing is mostly of dynamical nature. It is tied to the topographic shadowing effect related to changes in wind circulations, which causes as a predominant signal, an increase in precipitation on the upwind side of the mountains with respect to the main direction of the wind change.

In the summer, the topographic forcing is mostly of thermodynamical nature, being related to an increase in convective potential over the mountain peaks associated to high elevation heating and moistening. This process is similar to that found by Giorgi *et al.* (2016) for the Alps, with the important difference that it is of lower intensity because of the lower elevations and the smaller extent of the Carpathians compared to the Alps. In fact, while over the Alps, the topographic forcing actually reversed the sign of summer precipitation change over the mountain peaks (from negative to positive), in the Carpathians, it only attenuates the negative summer precipitation signal.

Our results thus confirm that even relatively small topographic features can modulate the local climatic precipitation change signal, with the characteristics of topography, and specifically elevation and orientation, playing a key role in this process. This implies that the representation of topography in climate models is a key element in the provision of robust precipitation information for application to local impact studies.

ACKNOWLEDGEMENTS

This paper was supported by the ÚNKP-19-4-ELTE-1202 New National Excellence Program of the Ministry for Innovation and Technology. The research leading to these results has also received funding from the Hungarian Academy of Sciences under the Premium Post-Doctoral Research Program and János Bolyai Research Scholarship. All data from EURO-CORDEX and Med-CORDEX modeling groups used in this work and CARPATCLIM, Database © European Commission—JRC 2013, along with *GTOPO30 data provided by the U.S. Geological Survey are acknowledged*. The data used in this work can be found at the following web sites: http://cordexesg.dmi.dk/esgf-web-fe/ (EURO-CORDEX), http://www.medcordex.eu/medcordex.php (Med-CORDEX), http://www.carpatclim-eu.org/pages/download/ (CARPATCLIM), and https://www.esrl.noaa.gov/psd/data/gridded/data.UDel_AirT_Precip.html (UDel).

ORCID

Csaba Torma https://orcid.org/0000-0002-4240-0788

REFERENCES

Bálint, M., Domisch, S., Engelhardt, C.H.M., Haase, P., Lehrian, S., Sauer, J., Theissinger, K., Pauls, S.U. and Nowak, C. (2011) Cryptic biodiversity loss linked to global climate change. *Nature Climate Change*, 1(6), 313–318.

Colin, J., Deque, M., Radu, R. and Somot, S. (2010) Sensitivity studies of heavy precipitations in limited area model climate simulation: influence of the size of the domain and the use of the spectral nudging technique. *Tellus A*, 62, 591–604. https://doi.org/10.1111/j.1600-0870.2010.00467.x.

Collins, W.J., Bellouin, N., Doutriaux-Boucher, M., Gedney, N., Halloran, P., Hinton, T., Hughes, J., Jones, C.D., Joshi, M., Liddicoat, S., Martin, G., O'Connor, F., Rae, J., Senior, C., Sitch, S., Totterdell, I., Wiltshire, A. and Woodward, S. (2011) Development and evaluation of an Earth-system model HadGEM2. *Geoscientific Model Development Discussions*, 4, 997–1062. https://doi.org/10.5194/gmdd-4-997-.

Déqué, M., Rowell, D., Lüthi, D., Giorgi, F., Christensen, J., Rockel, B., Jacob, D., Kjellström, E., De Castro, M. and van den Hurk, B. (2007) An intercomparison of regional climate simulations for Europe: assessing uncertainties in model projections. *Climate Change*, 81(1), 53–70.

Gao, X.J., Pal, J.S. and Giorgi, F. (2006) Projected changes in mean and extreme precipitation over the Mediterranean region from high resolution nested RCM simulations. *Geophysical Research Letters*, 33, L03706.

Giorgi, F., Shields Brodeur, C. and Bates, G.T. (1994) Regional climate change scenarios over the United States produced with a nested regional climate model. *Journal of Climate*, 7, 375–399.

Giorgi, F. and Coppola, E. (2010) Does the model regional bias affect the projected regional climate change? An analysis of global model projections. *Climatic Change Letters*, 100, 787–795.

Giorgi, F., Coppola, E., Solmon, F., Mariotti, L., Sylla, M.B., Bi, X., Elguindi, N., Diro, G.T., Nair, V., Giuliani, G., Turuncoglu, U. U., Cozzini, S., Guettler, I., O'Brien, T.A., Tawfik, A.B., Shalaby, A., Zakey, A.S., Steiner, A.L., Stordal, F., Sloan, L.C. and Brankovic, C. (2012) RegCM4: model description and preliminary results over multiple CORDEX domains. *Climate Research*, 52, 7–29. https://doi.org/10.3354/cr01018.

Giorgi, F., Torma, C., Coppola, E., Ban, N., Schär, C. and Somot, S. (2016) Enhanced summer convective rain at alpine high elevations in response to climate warming. *Nature Geoscience*, 9, 584–589. https://doi.org/10.1038/ngeo2761.

Hazeleger, W., et al. (2010) EC-EARTH: a seamless Earth system prediction approach in action. *Bulletin of the American Meteorological Society*, 91, 1357–1375. https://doi.org/10.1175/2010BAMS2877.1.

Jacob, D., van den Hurk, B.J.J.M., Andræ, U., Elgered, G., Fortelius, C., Graham, L.P., Jackson, S.D., Karstens, U., Köpken, C., Lindau, R., Podzun, R., Rockel, B., Rubel, F., Sass, B.H., Smith, R.N.B. and Yang, X. (2001) A comprehensive model intercomparison study investigating the water budget during the BALTEX-PIDCAP period. *Meteorology and Atmospheric Physics*, 77, 19–43. https://doi.org/10.1007/s007030170015.

Jacob, D., Petersen, J., Eggert, B., Alias, A., Christensen, O.B., Bouwer, L.M., Braun, A., Colette, A., Déqué, M., Georgievski, G., Georgopoulou, E., Gobiet, A., Menut, L., Nikulin, G., Haensler, A., Hempelmann, N., Jones, C., Keuler, K., Kovats, S., Kröner, N., Kotlarski, S., Kriegsmann, A., Martin, E., van Meijgaard, E., Moseley, C., Pfeifer, S., Preuschmann, S., Radermacher, C., Radtke, K., Rechid, D., Rounsevel, M., Samuelsson, P., Somot, S., Soussana, J.-F., Teichmann, C., Valentini, R., Vautard, R., Weber, B. and Yiou, P. (2014) EURO-CORDEX: new high resolution climate change projections for European impact research. *Regional Environmental Change*, 14, 563–578.

Jungclaus, J.H., Lorenz, S.J., Timmreck, C., Reick, C.H., Brovkin, V., Six, K., Segschneider, J., Giorgetta, M.A., Crowley, T.J., Pongratz, J., Krivova, N.A., Vieira, L.E., Solanki, S.K., Klocke, D., Botzet, M., Esch, M., Gayler, V., Haak, H., Raddatz, T.J., Roeckner, E., Schnur, R., Widmann, H., Claussen, M., Stevens, B. and Marotzke, J. (2010) Climate and carbon-cycle variability over the last millennium. *Ruti*, 6(5), 723.

Kozak, J., Gurung, B.A. and Ostapowicz, K. (Eds.). (2011) Research agenda for the Carpathians: 2010–2015. In: *Integrating Nature and Society Towards Sustainability, S4C Science for the Carpathians* (pp. 1–45). Krakow, Poland: Institute of Geography and Spatial Management, Jagiellonian University. http://www.carpathianconvention.org/tl_files/carpathiancon/Downloads/02Activities/2.1.10_S4CResearchStrategy.pdf.

Kuemmerle, T., Perzanowski, K., Chaskovskyy, O., Ostapowicz, K., Halada, L., Bashta, A.T., Kruhlov, I., Hostert, P., Waller, D.M. and Radeloff, V.C. (2010) European bison habitat in the Carpathian Mountains. *Biological Conservation*, 143(4), 908–916.

Kupiainen, M., et al. (2014) *Rossby Centre Regional Atmospheric Model, RCA4*. Norrköping, Sweden: Rossby Centre Newsletter. http://www.smhi.se/en/research/research-Departments/climate-research-rossby-centre2-552/1.16562.

Legates, D.R. and Willmott, C.J. (1990) Mean seasonal and spatial variability in gauge-corrected, global precipitation. *International Journal of Climatology*, 10, 111–127.

Meijgaard, E. et al., 2012: *Climate changes* (p. 44). De Bilt, Netherlands: KNMI (Royal Netherlands Meteorological Institute). https://edepot.wur.nl/312258.

Moss, R.H., Edmonds, J.A., Hibbard, K.A., Manning, M.R., Rose, S. K., van Vuuren, D.P., Carter, T.E., Emori, S., Kainuma, M., Kram, T., et al. (2010) The next generation of scenarios for climate change research and assessment. *Nature*, 463, 747–756.

Rockel, B., Will, A. and Hense, A. (2008) Special issue: regional climate modeling with COSMO-CLM (CCLM). *Meteorologische Zeitschrift*, 17, 347–348.

Ruti, P.M., Somot, S., Giorgi, F., Dubois, C., Flaounas, E., Obermann, A., Dell'Aquila, A., Pisacane, G., Harzallah, A., Lombardi, E., Ahrens, B., Akhtar, N., Alias, A., Arsouze, T., Aznar, R., Bastin, S., Bartholy, J., Béranger, K., Beuvier, J., Bouffies-Cloché, S., Brauch, J., Cabos, W., Calmanti, S., Calvet, J.-C., Carillo, A., Conte, D., Coppola, E., Djurdjevic, V., Drobinski, P., Elizalde-Arellano, A., Gaertner, M., Galàn, P., Gallardo, C., Gualdi, S., Goncalves, M., Jorba, O., Jordà, G., L'Heveder, B., Lebeaupin-Brossier, C., Li, L., Liguori, G., Lionello, P., Macià s, D., Nabat, P., Onol, B., Raikovic, B., Ramage, K., Sevault, F., Sannino, G., Struglia, M.V., Sanna, A., Torma, C. and Vervatis, V. (2016) MED-CORDEX initiative for Mediterranean climate studies. *Bulletin of the American Meteorological Society*, 97, 1187–1208. https://doi.org/10.1175/BAMS-D-14-00176.1.

Szalai, S., Auer, I., Hiebl, J., Milkovich, J., Radim, T., Stepanek, P., Zahradnicek, P., Bihari, Z., Lakatos, M., Szentimrey, T., Limanowka, D., Kilar, P., Cheval, S., Deak, Gy., Mihic, D., Antolovic, I., Mihajlovic, V., Nejedlik, P., Stastny, P., Mikulova, K., Nabyvanets, I., Skyryk, O., Krakovskaya, S., Vogt, J., Antofie, T., and Spinoni, J., 2013: *Climate of the Greater Carpathian Region*. Final Technical Report. https://surfobs.climate.copernicus.eu/dataaccess/access_carpatclim_indices.php.

Torma, C. S., Giorgi, F., and Coppola, E. (2015) Added value of regional climate modeling over areas characterized by complex terrain-Precipitation over the Alps. *Journal of Geophysical Research: Atmospheres*, 120, 3957–3972. https://doi.org/10.1002/2014JD022781.

UNEP. (2007) *Carpathian Environmental Outlook—KEO2007*. Geneva, Switzerland: United Nations Environment Programme, p. 236.

Voldoire, A., Sanchez-Gomez, E., Salas y Mélia, D., Decharme, B., Cassou, C., Sénési, S., Valcke, S., Beau, I., Alias, A., Chevallier, M., Déqué, M., Deshayes, J., Douville, H., Fernandez, E., Madec, G., Maisonnave, E., Moine, M.P., Planton, S., Saint-Martin, D., Szopa, S., Tyteca, S., Alkama, R., Belamari, S., Braun, A., Coquart, L. and Chauvin, F. (2012) The CNRMCM5 global climate model: description and basic evaluation. *Climate Dynamics*, 40, 2091–2121. https://doi.org/10.1007/s00382-011-1259-y.

SUPPORTING INFORMATION

Additional supporting information may be found online in the Supporting Information section at the end of this article.

How to cite this article: Torma C, Giorgi F. On the evidence of orographical modulation of regional fine scale precipitation change signals: The Carpathians. *Atmos Sci Lett*. 2020;e967. https://doi.org/10.1002/asl.967